



Assessing Inflammation in Acute Intracerebral Hemorrhage with PK11195 PET and Dynamic Contrast-Enhanced MRI

DOI:

[10.1111/jon.12477](https://doi.org/10.1111/jon.12477)

Document Version

Accepted author manuscript

[Link to publication record in Manchester Research Explorer](#)

Citation for published version (APA):

Abid, K. A., Sobowale, O. A., Parkes, L. M., Naish, J., Parker, G. J. M., du Plessis, D., Brough, D., Barrington, J., Allan, S. M., Hinz, R., & Parry-Jones, A. R. (2018). Assessing Inflammation in Acute Intracerebral Hemorrhage with PK11195 PET and Dynamic Contrast-Enhanced MRI. *Journal of Neuroimaging*, 28(2), 158-161. <https://doi.org/10.1111/jon.12477>

Published in:

Journal of Neuroimaging

Citing this paper

Please note that where the full-text provided on Manchester Research Explorer is the Author Accepted Manuscript or Proof version this may differ from the final Published version. If citing, it is advised that you check and use the publisher's definitive version.

General rights

Copyright and moral rights for the publications made accessible in the Research Explorer are retained by the authors and/or other copyright owners and it is a condition of accessing publications that users recognise and abide by the legal requirements associated with these rights.

Takedown policy

If you believe that this document breaches copyright please refer to the University of Manchester's Takedown Procedures [<http://man.ac.uk/04Y6Bo>] or contact uml.scholarlycommunications@manchester.ac.uk providing relevant details, so we can investigate your claim.





Assessing inflammation in acute intracerebral hemorrhage with PK11195 PET and dynamic contrast-enhanced MRI

Journal:	<i>Journal of Neuroimaging</i>
Manuscript ID	JON-17-5003.R1
Wiley - Manuscript type:	Short Communication
Date Submitted by the Author:	19-Sep-2017
Complete List of Authors:	<p>Abid, Kamran; University of Manchester, Division of Neuroscience and Experimental Psychology; Salford Royal Hospital , Greater Manchester Neurosciences Centre</p> <p>Sobowale, Oluwaseun; University of Manchester, Division of Neuroscience and Experimental Psychology; Salford Royal Hospital , Greater Manchester Neurosciences Centre</p> <p>Parkes, Laura; University of Manchester, Division of Neuroscience and Experimental Psychology</p> <p>Naish, Josephine; University of Manchester Institute of Cardiovascular Sciences</p> <p>Parker, Geoff; University of Manchester, Division of Informatics, Imaging and Data Sciences; Bioxydyn Limited, Rutherford House, Pencroft Way</p> <p>Duplessis, Daniel; Salford Royal Hospital , Greater Manchester Neurosciences Centre</p> <p>Brough, Daniel; University of Manchester, Division of Neuroscience and Experimental Psychology</p> <p>Barrington, Jack; University of Manchester Institute of Cardiovascular Sciences</p> <p>Allan, Stuart; University of Manchester, Division of Neuroscience and Experimental Psychology</p> <p>Hinz, Rainer; The University of Manchester , Wolfson Molecular Imaging Centre</p> <p>Parry-Jones, Adrian; University of Manchester Institute of Cardiovascular Sciences; Salford Royal Hospital , Greater Manchester Neurosciences Centre</p>
Keywords:	intracerebral haemorrhage, inflammation, blood-brain barrier, magnetic resonance imaging, positron emission tomography
Subject Area:	Imaging Techniques < NEUROIMAGING, Magnetic Resonance Imaging (MRI) < Magnetic Resonance (MR) < Imaging Techniques < NEUROIMAGING, Positron Emission Tomography (PET) < Imaging Techniques < NEUROIMAGING

1
2
3
4
5
6
7
8
9
10
11
12
13
14
15
16
17
18
19
20
21
22
23
24
25
26
27
28
29
30
31
32
33
34
35
36
37
38
39
40
41
42
43
44
45
46
47
48
49
50
51
52
53
54
55
56
57
58
59
60

SCHOLARONE™
Manuscripts

For Peer Review

Assessing inflammation in acute intracerebral hemorrhage with PK11195 PET and dynamic contrast-enhanced MRI

Imaging inflammation in acute intracerebral hemorrhage: a combined [¹¹C]-(R)-PK11195 PET and DCE-MRI study

Kamran A Abid PhD^{1,3*}, Oluwaseun A Sobowale MRCS^{1,3*}, Laura M Parkes PhD¹, Josephine Naish PhD¹, Geoff JM Parker PhD^{1,2}, Daniel du Plessis FRCPath³, David Brough PhD¹, Jack Barrington BSc¹, Stuart M Allan PhD¹, Rainer Hinz PhD¹, Adrian R Parry-Jones PhD^{1,3}

¹Faculty of Biology, Medicine and Health, The University of Manchester, Manchester, UK;

²Bioxydyn Limited, Manchester, UK; ~~Rutherford House, Peneroft Way, Manchester, M15 6SZ, UK;~~

³Greater Manchester Neurosciences Centre, Salford Royal NHS Foundation Trust, ~~Salford~~Manchester, UK.

*Contributed equally

Corresponding Author:

Dr A.R. Parry-Jones

Salford Royal NHS Foundation Trust, Stott Lane

Salford, M6 8HD, UK

E-mail: adrian.parry-jones@manchester.ac.uk

Tel: +44 161 2064458

Fax: +44 161 7076534

Running title: Multimodality imaging of brain inflammation in ICH

Key words: Intracerebral haemorrhage, inflammation, blood-brain barrier, magnetic resonance imaging, positron emission tomography

Formatted: Default Paragraph Font, Font: (Default) +Body (Cambria), 11 pt, English (U.K.)

1
2
3
4
5
6
7
8
9
10
11
12
13
14
15
16
17
18
19
20
21
22
23
24
25
26
27
28
29
30
31
32
33
34
35
36
37
38
39
40
41
42
43
44
45
46
47
48
49
50
51
52
53
54
55
56
57
58
59
60

Acknowledgements ~~and none~~

Disclosures: none.

Formatted: Line spacing: Double

For Peer Review

Abstract

Background and purpose:

Studies in animal models ~~have suggested~~suggest that inflammation is a major contributor to secondary injury after intracerebral haemorrhage (ICH). Direct, non-invasive monitoring of inflammation in the human brain after ICH will facilitate early-phase development of anti-inflammatory treatments. We sought to investigate the feasibility of multi-modality brain imaging in subacute ICH.

Methods:

Acute ICH patients were recruited to undergo multiparametric ~~magnetic resonance imaging~~MRI (including dynamic contrast enhanced measurement of blood-brain barrier transfer constant (K^{trans}) and ~~positron emission tomography~~ (PET) with [^{11}C]-(*R*)-PK11195. [^{11}C]-(*R*)-PK11195 binds to the translocator protein 18 kDa (TSPO), which is rapidly upregulated in activated microglia. Circulating inflammatory markers were measured at the time of PET.

Results:

Five patients were recruited to this feasibility study with imaging ~~performed~~ between 5 and 16 days after onset. Etiologies included hypertension-related small vessel disease, cerebral amyloid angiopathy (CAA), cavernoma and arteriovenous malformation (AVM). [^{11}C]-(*R*)-PK11195 binding was low in all hematomas and two (patient 2 (probable CAA) and patient 4 (AVM)) showed widespread increase in binding in the perihematoma region vs. contralateral. All had increased K^{trans} in the perihematoma region (mean difference = $2.2 \times 10^{-3} \text{ min}^{-1}$; SD = $1.6 \times 10^{-3} \text{ min}^{-1}$) vs. contralateral. Two cases (patients 1 (cavernoma) and 4

1
2
3
4
5
6
7
8
9
10
11
12
13
14
15
16
17
18
19
20
21
22
23
24
25
26
27
28
29
30
31
32
33
34
35
36
37
38
39
40
41
42
43
44
45
46
47
48
49
50
51
52
53
54
55
56
57
58
59
60

(AVM) had delayed surgery (three and 12-months post-onset, [respectively](#)) with biopsies showing intense microglial activation in perilesional tissue.

Conclusions:

Our study demonstrates for the first time the feasibility of performing complex multi-modality brain imaging for non-invasive monitoring of neuroinflammation for this severe stroke subtype. ~~These techniques will be useful tools in developing anti-inflammatory treatments for clinical ICH.~~

For Peer Review

Introduction

After intracerebral hemorrhage (ICH), extravasation of blood leads to immediate physical tissue injury. Secondary damage ensues over hours and days, mediated by a cascade of molecular and cellular events involving the toxic effects of blood components and sterile inflammation.^{1[1]} Within hours of onset, microglia become activated taking on a pro-inflammatory phenotype, releasing cytokines and chemokines that activate astrocytes and endothelial cells causing blood-brain barrier (BBB) breakdown [\(alongside the direct effects of the ICH\)](#), recruitment of circulating leukocytes, and exacerbation of perihematomal edema.^{2[2]} Previous clinical studies in ICH have largely focused on peripheral inflammatory markers showing associations between fever, elevated white blood cell count, interleukin-6 (IL-6), C-reactive protein (CRP), and fibrinogen on admission and worse sub-acute and long-term outcomes.^{3[3]} These clinical studies demonstrate the importance of the systemic inflammatory response, but provide no information on processes within the brain, where inflammation contributes directly to secondary injury. Given the growing interest in modulating inflammation in acute ICH and the failure in ischemic stroke to translate findings from animal models, a means of studying inflammation in the intact human brain after ICH is urgently required.

Using advanced multimodality imaging, it is possible to estimate the extent and distribution of microglial activation and BBB breakdown. When activated, microglia express the translocator protein 18 kDa (TSPO), normally present at very low levels in the central nervous system. [¹¹C]-(R)-PK11195 binds to TSPO and has been used for [positron emission tomography \(PET\)](#) studies of acute ischemic stroke,^{4[4]} but *in vivo* imaging of microglial activation in ICH has not been previously described. Using [magnetic resonance imaging \(MRI\)](#) and [computed tomography \(CT\)](#) dynamic contrast enhanced (DCE) techniques, two previous studies have quantified BBB breakdown after ICH.^{5,6[5,6]} Combining this

1
2
3
4
5
6
7 technique with [¹¹C]-(R)-PK11195 PET will provide a more complete picture of the
8
9 inflammatory response and allow an understanding of the extent that BBB breakdown co-
10
11 localizes with microglial activation with important implications for the delivery of an anti-
12
13 inflammatory drug to the brain. Our aim was to demonstrate the feasibility of combining
14
15 these techniques in patients during the acute stage of ICH and describe hypothesis-generating
16
17 preliminary findings.

21 22 Methods

23
24 Patients between 4 and 28 days after onset of acute, spontaneous ICH were recruited from
25
26 Salford Royal NHS Foundation Trust (Salford, UK) between 05/12/12 and 28/03/2014,
27
28 following appropriate approvals. We excluded patients if they had a contraindication to MRI,
29
30 were pregnant or breast feeding, had significant renal impairment, had an acute neurosurgical
31
32 procedure performed or planned or who were taking medications which were likely to
33
34 interfere with [¹¹C]-(R)-PK11195 binding. MRI was performed on a Philips 3 T Achieva
35
36 scanner (Salford Royal Hospital) with an 8 channel head coil. PET scans were performed
37
38 within 4 days of MRI on a High Resolution Research Tomograph (Siemens/CTI) PET
39
40 scanner (Wolfson Molecular Imaging Centre, University of Manchester). Venous blood was
41
42 collected at recruitment (where possible) and immediately prior to the PET scan for
43
44 measurement of key inflammatory mediators (CRP, IL-6, interleukin-1 (IL-1); see online
45
46 supplement for immunoassay methods).

47
48 MRI included T₁-weighted volumetric Fast Field Echo (T₁-FFE) imaging, T₂-weighted fluid
49
50 attenuated inversion recovery (FLAIR) imaging and T₁-weighted DCE-MRI. Parametric
51
52 maps of the blood-brain barrier transfer constant (K^{trans}) were generated from DCE-MRI data
53
54 using an uptake model (details of MRI acquisition and analysis in online supplementary
55

1
2
3
4
5
6
7 methods). PET data were analyzed as previously described.^{7,77} In brief, iterative ordered
8 subset expectation maximization 3D method was used to reconstruct a quantitative series of
9 dynamic images from the [60 min](#) PET emission scan. A reference tissue input function was
10 extracted from cerebellar grey matter in order to generate parametric maps of binding
11 potential BP_{ND} using the simplified reference tissue model. Using SPM (version 8), all maps
12 and images were co-registered to the T_1 -weighted volume MRI. The T_1 -weighted volume
13 image was segmented into grey matter and white matter probability maps and a maximum
14 probability brain atlas^{8,81} was warped in to individual space. Two regions of interest (ROI)
15 were defined manually from the T_1 -weighted and FLAIR images, representing hematoma and
16 perihematomal edema. Corresponding ROIs in the contralateral brain region were generated
17 by flipping the ipsilateral ROIs about the midline in the axial plane excluding any non-brain
18 tissue. The mean binding potential (BP_{ND}) of [^{11}C]-(*R*)-PK11195 and K^{trans} within each ROI
19 was then extracted from the parametric maps using Analyze version 12.0 (Mayo Clinic).
20
21
22
23
24
25
26
27
28
29
30
31
32
33
34

35 Results

36
37 Five patients with acute ICH underwent research brain imaging between 5 and 25 days after
38 onset as part of this feasibility study (Table 1). All patients tolerated the scans without
39 difficulty except patient 3, who was unable to complete the last 22 min of the 60 min
40 emission PET scan and was the only one to undergo both scans on one day. Etiologies
41 [confirmed using appropriate clinical imaging](#) included a cavernous angioma, an arteriovenous
42 malformation (Figure 1), probable cerebral amyloid angiopathy and small vessel disease due
43 to chronic hypertension. [^{11}C]-(*R*)-PK11195 binding was low in all hematomas. Patients 2 &
44 4 showed increased [^{11}C]-(*R*)-PK11195 binding both within the perihematomal edema
45 volume (~~0.24 and 0.06 respectively, vs. contralateral~~) and the ipsilateral brain region (~~0.13 &~~
46
47
48
49
50
51
52
53
54
55

1
2
3
4
5
6
7 [0.12 respectively, vs. contralateral; Figure 2\). Patients 1 and 4 underwent surgery at 3 and 12](#)
8 [months, respectively, with perilesional tissue demonstrating intense microglial activation.](#)

9
10 Analyses of DCE-MRI data show increases in K^{trans} in the perihematomal edema volume
11 (mean difference = $2.2 \times 10^{-3} \text{ min}^{-1}$; SD = $1.6 \times 10^{-3} \text{ min}^{-1}$) in all 5 patients relative to the
12 contralateral. Visual inspection of images (Figure 2) consistently demonstrates a clear ring of
13 increased K^{trans} adjacent to the outer border of the hematoma. No pattern is suggested for a
14 relationship between circulating inflammatory markers and imaging, ~~though for all cases,~~
15 [CRP was lower at the time of PET scanning than at recruitment.](#)

22 23 24 Discussion

25
26 Our small study is the first to show imaging of microglial activation with PET after ICH and
27 demonstrates the feasibility of performing complex multimodality brain imaging after acute
28 ICH. However, we found that performing PET and MR scans on different days may improve
29 successful study completion. All patients show clear ring-shaped BBB breakdown in the
30 outer border of the hematoma, suggesting that delivery of treatments with limited transfer
31 across the intact BBB may be enhanced in acute ICH. We observed a heterogeneous pattern
32 of [^{11}C]-(*R*)-PK11195 binding, with only two patients demonstrating enhanced binding
33 around the hematoma. In neither case was the binding closely co-located with the BBB
34 disruption, suggesting that factors other than microglial activation may drive BBB
35 breakdown after ICH, an observation that should be investigated further in future studies.

36
37
38 [Late perilesional biopsies in two patients did show intense microglial activation, but only one](#)
39 [had enhanced \[\$^{11}\text{C}\$ \]-\(*R*\)-PK11195 binding acutely. The long delay between PET and biopsies](#)
40 [makes it difficult to interpret this disparity.](#)

51 52 53 Summary/Conclusions

We have demonstrated the feasibility of performing complex multimodality imaging to track the inflammatory response after ICH. This will be a vital tool in investigating this promising therapeutic target with potential use in early phase proof-of-concept clinical trials.

References

- [1] Gong C, Hoff JT, Keep RF. Acute inflammatory reaction following experimental intracerebral hemorrhage in rat. *Brain Research*. 2000;871:57-65.
- [2] Askenase MH, Sansing LH. Stages of the inflammatory response in pathology and tissue repair after intracerebral hemorrhage. *Seminars in Neurology*. 2016;36:288-97.
- [3] Di Napoli M, Godoy DA, Campi V, et al, Masotti L, Smith CJ, Jones ARP, Hopkins SJ, Slevin M, Papa F, Mogoanta L, Pirici D, Wagner AP. C-reactive protein in intracerebral hemorrhage: Time course, tissue localization, and prognosis. *Neurology*. 2012;79:690-9.
- [4] Gerhard A, Schwarz J, Myers R, Wise R, Banati RB. Evolution of microglial activation in patients after ischemic stroke: a C-11 (R)-PK11195 PET study. *Neuroimage*. 2005;24:591-5.
- [5] McCourt R, Gould B, Kate M, et al, Asdaghi N, Kosior JC, Coutts S, Hill MD, Demehuk A, Jeerakathil T, Emery D, Butcher KS. Blood-brain barrier compromise does not predict perihematoma edema growth in intracerebral hemorrhage. *Stroke*. 2015;46:954-60.
- [6] Aksoy D, Bammer R, Mlynash M, et al, Venkatasubramanian C, Eyingorn I, Snider RW, Gupta SN, Narayana R, Fischbein N, Wijman CAC. Magnetic resonance imaging profile of blood-brain barrier injury in patients with acute intracerebral hemorrhage. *Journal of the American Heart Association*. 2013;2:e000161.
- [7] Su ZJ, Herholz K, Gerhard A, et al, Roncaroli F, Du Plessis D, Jackson A, Turkheimer F, Hinz R. C-11 (R)-PK11195 tracer kinetics in the brain of glioma patients and a comparison of two referencing approaches. *European Journal of Nuclear Medicine and Molecular Imaging*. 2013;40:1406-19.
- [8] Hammers A, Chen CH, Lemieux L, et al, Allom R, Vossos S, Free SL, Myers R, Brooks DJ, Duncan JS, Koeppe MJ. Statistical neuroanatomy of the human inferior frontal gyrus and probabilistic atlas in a standard stereotaxic space. *Human Brain Mapping*. 2007;28:34-48.

Formatted: Font: (Default) Times New Roman, 12 pt, English (U.S.)

Field Code Changed

Formatted: Font: (Default) Times New Roman, 12 pt, Not Italic, English (U.S.)

Formatted: Font: (Default) Times New Roman, 12 pt, English (U.S.)

Formatted: Font: (Default) Times New Roman, 12 pt

Formatted: Font: (Default) Times New Roman, 12 pt, English (U.S.)

Formatted: Font: (Default) Times New Roman, 12 pt, Not Italic, English (U.S.)

Formatted: Font: (Default) Times New Roman, 12 pt, English (U.S.)

Formatted: Font: (Default) Times New Roman, 12 pt

Formatted: Font: (Default) Times New Roman, 12 pt, English (U.S.)

Formatted: Font: (Default) Times New Roman, 12 pt

Formatted: Font: (Default) Times New Roman, 12 pt, English (U.S.)

Formatted: Font: (Default) Times New Roman, 12 pt

Formatted: Font: (Default) Times New Roman, 12 pt, English (U.S.)

Formatted: Font: (Default) Times New Roman, 12 pt

Formatted: Font: (Default) Times New Roman, 12 pt, English (U.S.)

Formatted: Font: (Default) Times New Roman, 12 pt, Not Italic, English (U.S.)

Formatted: Font: (Default) Times New Roman, 12 pt, English (U.S.)

Formatted: Font: (Default) Times New Roman, 12 pt, English (U.S.)

Formatted: Font: (Default) Times New Roman, 12 pt

Formatted: Font: (Default) Times New Roman, 12 pt, English (U.S.)

Formatted: Font: (Default) Times New Roman, 12 pt, Not Italic, English (U.S.)

Formatted: Font: (Default) Times New Roman, 12 pt, English (U.S.)

Formatted ... [1]

Formatted ... [2]

Formatted ... [3]

Formatted ... [4]

Formatted ... [5]

Formatted ... [6]

Formatted ... [7]

Table 1. Baseline characteristics, inflammatory markers and imaging data.

	Patient 1	Patient 2	Patient 3	Patient 4	Patient 5
Baseline Characteristics					
Age (years)	30	63	85	43	46
Sex	Female	Male	Female	Male	Male
GCS at presentation	14	15	15	14	15
ICH etiology	Cavernous angioma ²	Probable CAA ¹	Primary undetermined	Arteriovenous malformation ²	Chronic hypertension
ICH location	Right temporal	Right occipital	Left cerebellar	Left parietal	Left lentiform
ICH volume (ml)	6.1	6.7	8.5	30.0	7.1
PHE volume (ml)	4.3	6.9	5.2	15.9	4.4
PET scan (days post-onset)	7	11	25	16	10
MR scan (days post-onset)	9	10	25	12	7
Inflammatory mediators					
IL-1 β					
baseline (pg/ml)	-	-	0.56	0.63	0.81
PET scan (pg/ml)	0.81	1.07	1.90	1.94	2.01
IL-6					
baseline (pg/ml)	-	-	7.77	2.35	2.73
PET scan (pg/ml)	3.82	<0.012	4.29	1.5	4.47
IL-8					
baseline (pg/ml)	-	-	16.97	16.12	35.16
PET scan (pg/ml)	11.53	4.84	15.77	10.66	25.59
CRP					
baseline (mg/l)	-	-	2.80	4.32	4.54
PET scan (mg/l)	0.472	0.598	0.862	0.85	1.64
DCE-MRI parameters					
Mean K^{trans} ($\times 10^{-3} \text{ min}^{-1}$)					
Perihematoma edema					
Ipsilateral	1.8	5.7	2.1	2.9	2.2
Contralateral	0.4	0.7	1.0	1.0	0.6
Ipsilateral - contralateral	1.4	5.0	1.0	1.9	1.6

Table 1: Baseline characteristics, inflammatory markers and imaging data.¹Based on

modified Boston criteria; ²Confirmed on histology at later surgical resection. **ICH =**

intracerebral haemorrhage. pg = picogram, ml = millilitre, l = litre, mg = milligram, GCS =

Formatted: Font: Bold, Underline

Formatted: Font: Bold, Underline

Formatted: Underline

Formatted: Font: Bold, Font color: Background 1

Formatted Table

1
2
3
4
5
6
7 Glasgow Coma Scale, PHE = peri-haematoma edema, CRP = C-reactive protein, DCE =
8 dynamic contrast-enhanced, K^{trans} = volume transfer constant, IL = interleukin, CAA =
9 cerebral amyloid angiopathy.
10
11
12

13
14
15
16 Figure legends

17
18 Figure 1: Cluster of differentiation 68CD68 immunostaining (original magnification x400)
19 demonstrates diffuse microglial activation (2a) in patient 1 (suspected cavernoma) and
20 activated microglia and phagocytic activity (2b) in patient 4 (arteriovenous
21 malformationAVM).
22
23
24
25
26

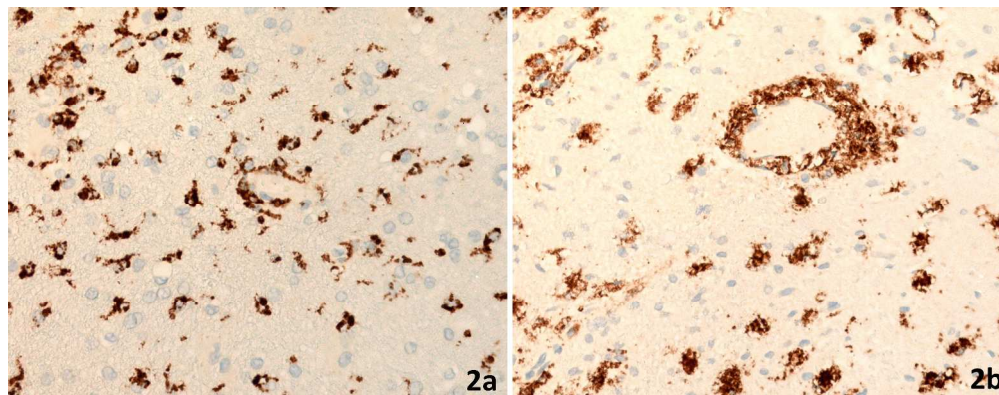
Formatted: Font: (Default) Times New Roman, 12 pt

27
28
29 Figure 2: Representative parametric maps of [^{11}C]-(*R*)-PK11195 PET binding potential
30 (BP_{ND}) (superimposed on to T₁-weighted images) and volume transfer constant (K^{trans} -) with
31 Fluid-attenuated inversion recovery (FLAIR) FLAIR images from each patient with regions
32 of interestROIs for hematoma (green) and edema (red). Increased [^{11}C]-(*R*)-PK11195 binding
33 is indicated in patients 2&4 by arrows.
34
35
36
37
38
39
40
41
42
43
44
45
46
47
48
49
50
51
52
53
54
55

Formatted: Font: (Default) Times New Roman, 12 pt

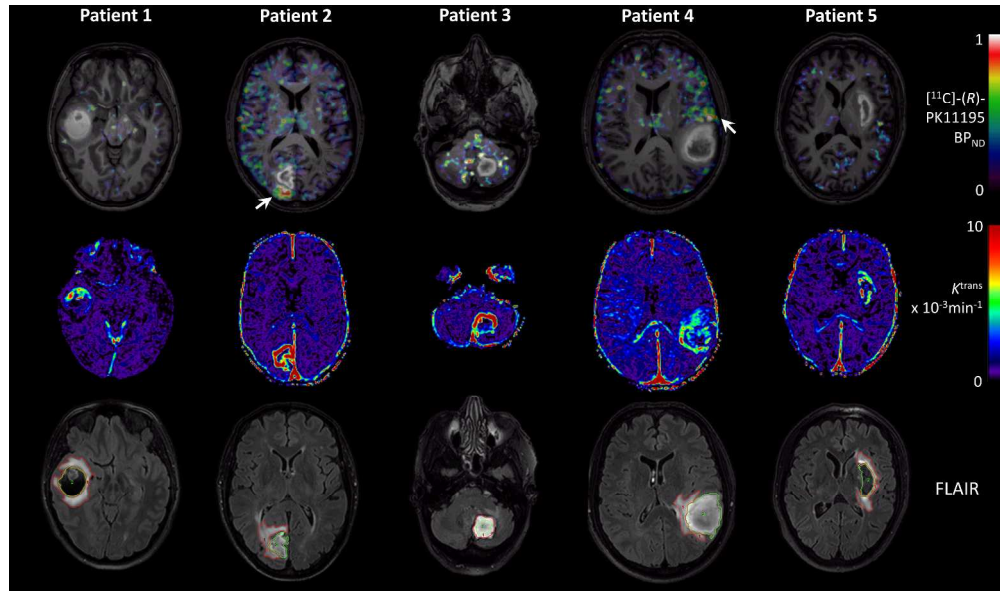
1
2
3
4
5
6
7
8
9
10
11
12
13
14
15
16
17
18
19
20
21
22
23
24
25
26
27
28
29
30
31
32
33
34
35
36
37
38
39
40
41
42
43
44
45
46
47
48
49
50
51
52
53
54
55
56
57
58
59
60

For Peer Review



Cluster of differentiation 68 immunostaining (original magnification x400) demonstrates diffuse microglial activation (2a) in patient 1 (suspected cavernoma) and activated microglia and phagocytic activity (2b) in patient 4 (arteriovenous malformation).

1278x503mm (96 x 96 DPI)



Representative parametric maps of $[^{11}\text{C}]-(R)\text{-PK11195}$ PET binding potential (BPND) (superimposed on to T1-weighted images) and volume transfer constant (k^{trans}) with Fluid-attenuated inversion recovery (FLAIR) images from each patient with regions of interest for hematoma (green) and edema (red). Increased $[^{11}\text{C}]-(R)\text{-PK11195}$ binding is indicated in patients 2&4 by arrows.

1280x750mm (96 x 96 DPI)